RZ 3939 (# ZUR1807-036) 07/11/2018
Physical Sciences 20 pages

# Research Report

## Controlled Fragmentation of Single Molecules with Atomic Force Microscopy by Employing Doubly Charged States

Shadi Fatayer*, Nikolaj Moll*, Sara Collazos[#], Dolores Pérez[#], Enrique Guitián[#], Diego Peña[#], Leo Gross*, Gerhard Meyer*

*IBM Research – Zurich
8803 Rüschlikon
Switzerland

[#]Centro de Investigaci on en Qu mica Biol oxica e Materiais
Moleculares (CIQUS) and Departamento de Qu mica Org anica,
Universidade de Santiago de Compostela,
Santiago de Compostela 15782, Spain

This is the accepted version of the article published by the American Physical Society:
Shadi Fatayer, Nikolaj Moll, Sara Collazos, Dolores Pérez, Enrique Guitián, Diego Peña, Leo Gross, and Gerhard Meyer
"Controlled Fragmentation of Single Molecules with Atomic Force Microscopy by Employing Doubly Charged States"

Phys. Rev. Lett. 121(22) (2018) DOI:10.1103/PhysRevLett.121.226101

# Controlled fragmentation of single molecules with atomic force microscopy by employing doubly charged states

Shadi Fatayer,[1,*] Nikolaj Moll,[1] Sara Collazos,[2] Dolores Pérez,[2]
Enrique Guitián,[2] Diego Peña,[2] Leo Gross,[1,†] and Gerhard Meyer[1]

[1]*IBM Research – Zurich, Säumerstrasse 4, 8803 Rüschlikon, Switzerland*

[2]*Centro de Investigación en Química Biolóxica e Materiais Moleculares (CIQUS) and Departamento de Química Orgánica, Universidade de Santiago de Compostela, Santiago de Compostela 15782, Spain*

(Dated: October 3, 2018)

## Abstract

By atom manipulation we performed on-surface chemical reactions of a single molecule on a multilayer insulating film using non-contact atomic force microscopy (AFM). The single-electron sensitivity of AFM allows following the addition of single electrons to the molecule and the investigation of the reaction products. By performing a novel strategy based on long lived doubly-charged states a single molecule is fragmented. The fragmentation can be reverted by again changing the charge-state of the system, characterizing a reversible reaction. The experimental results in addition with density-functional theory provide insight into the charge-states of the different products and reaction pathways. Similar molecular systems could be used as charge-transfer units and to induce reversible chemical reactions.

PACS numbers: 68.37.Ps, 68.35.-p, 68.43.-h, 82.30.Qt, 82.37.Gk

On-surface intramolecular chemical reactions involve the dissociation, formation and rearrangement of covalent bonds within molecules on surfaces [1–4]. With scanning probe microscopy, reactions of different molecular systems on surfaces have been thoroughly investigated [5–11]. On metals and semiconductors, where the scanning tunneling microscope (STM) can be used, usually currents on the order of nano- to picoamperes are required to inelastically excite particular vibrational modes to initiate a reaction [5, 12, 13]. Also on ultra-thin insulating layers, as for example bilayer NaCl on Cu, tunneling currents in the picoampere regime are accessible and often employed for tip-induced chemical reactions [14, 15]. Insulating films are important for avoiding current leakage in single-electron devices. However, there are challenges in studying on-surface chemistry on insulators. With increasing thickness of the insulating film the maximum accessible tunneling current decreases exponentially [16], until in the limit of bulk insulators no tunneling current between tip and sample is possible within the insulator gap. Hence, one cannot apply a current between tip and substrate through the molecule to promote chemical reactions. For this reason no molecular reactions have been demonstrated by atom manipulation on bulk insulators to date. In addition, only few examples of on-surface chemistry by thermal annealing on defect-free insulators have been reported to date [3, 17–21].

Novel strategies are desired to perform chemical reactions on insulators by atom manipulation. The atomic force microscope (AFM), capable of operating on insulators, offers the spatial resolution needed [22]. Atomic manipulation and controlling the positions of adatoms by AFM have been demonstrated [23–25]. With the proven single-electron sensitivity [22, 26, 27], AFM is the ideal tool for following chemical reactions based on employing different charge states of adsorbates on insulators. In addition, employing multiple charge states provides different reaction pathways for novel on-surface syntheses. Here, we present the reversible dissociation of 10,11-diiodonaphtho[1,2,3,4-*ghi*]perylene (DINP) adsorbed on an insulator. AFM is used for probing the attachment/detachment of single electrons to DINP by imaging the products and evaluating the charge states of the products.

We show that singly negatively charged DINP is stable, as is the singly positively charged DINP on NaCl. Upon attachment of two electrons, the doubly negatively charged DINP fragments into an aryne and two iodide ions. The dissociation is reversible. By removing two electrons from the dissociated products, a neutral DINP molecule is reestablished. Density-functional theory (DFT) calculations support the hypothesized individual charges of the

fragmented products.

The measurements were performed in a combined STM/AFM that utilizes a qPlus tuning fork sensor [28], operated in the frequency-modulation mode [29]. An oscillation amplitude $A$ varying between 4 to 6 Å was chosen to increase the signal-to-noise ratio in detecting single charges. The microscope was operated under ultrahigh vacuum ($p \approx 10^{-11}$ mbar) and low temperature ($T \approx 5$ K) conditions. Voltages were applied to the sample. As substrate we used a Cu(111) single crystal covered with different layer thicknesses of NaCl. One part of the crystal is covered with NaCl bilayer islands for tip preparation, the other part was covered with a NaCl film of more than 10 monolayers thick, precluding charge transfer to the metal below on time-scales of the experiments [16]. Molecules were evaporated onto the cold (10 K) sample. Cu terminated AFM tips were prepared by controlled indentation into the copper substrate. Selected AFM tips had a $\Delta f$ of less than -1 Hz at tunneling currents of 1 pA and 0.2 V while on bilayer NaCl and a maximum $\Delta f$ of 3 Hz while at 1 pA and 2 V. Such tips allowed resolution on charge-state transitions of the reactants on multilayer thick films. As the tips are Cu terminated, no atomic spatial resolution can be achieved on molecules [30].

By employing a multilayer insulating film, the only possible electron-transfer pathway is between the tip and DINP, as sketched in Fig. 1 (a). DINP, whose chemical structure is displayed in Fig. 1 (b), is imaged on the multilayer NaCl film by AFM with a metal tip, in constant-height mode. The AFM image reveals two overlapping lobes (Fig. 1 (c)). The larger lobe corresponds to the hydrocarbon part of DINP whereas the smaller lobe corresponds to its two iodines. These assignments are corroborated by the comparison to the contrast of DINP on bilayer NaCl/Cu(111) obtained with high-resolution AFM images using CO-functionalized tips [31].

To investigate the stability of DINP upon electron attachment and detachment, a $\Delta f\,(V)$ spectrum is obtained: the tip is placed above of the molecule at constant height and the sample voltage is swept accordingly to reach the desired charge state of the molecule. The tip height for the $\Delta f\,(V)$ spectra is set 5 Å closer than the set point value of $\Delta f$ = -0.5 Hz and $V$ = 0.4 V above the NaCl surface. Upon accessing the appropriate molecular energy level, an electron can be transferred between tip and molecule. The change in charge state is observed as a transition from one $\Delta f\,(V)$ parabola to another one, typically giving rise to a step in the $\Delta f\,(V)$ spectrum [26, 32]. Here, sweeping the sample voltage to 2 V, the lowest unoccupied

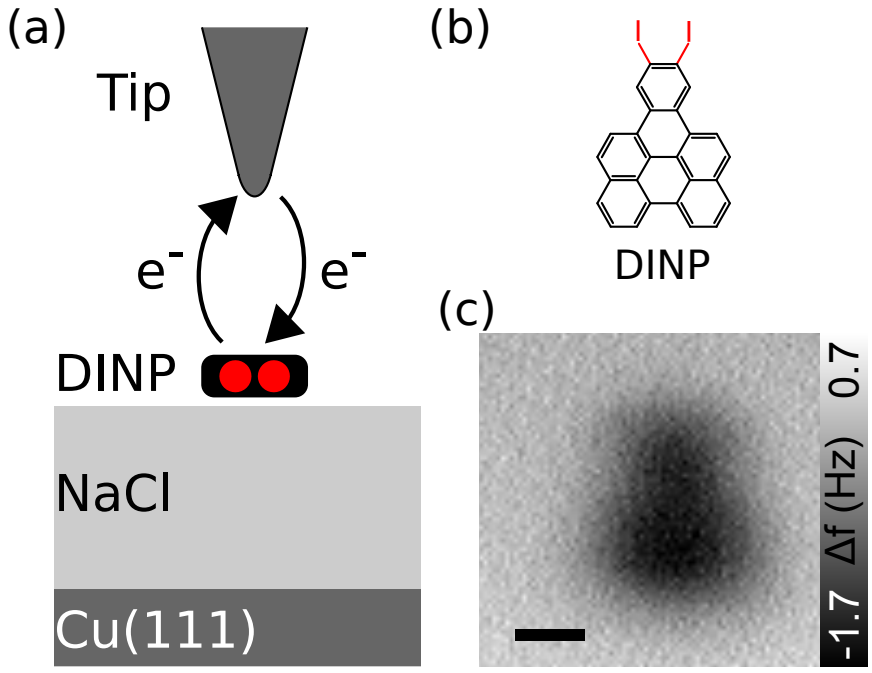


FIG. 1. **(a)** Schematic of the experimental arrangement. Because of the NaCl thickness being larger than 10 monolayers, electron transfer is possible only between tip and molecule. **(b)** DINP model. **(c)** Constant-height AFM image of DINP on NaCl ($A = 4\,\text{Å}$ and $V = 2.3\,\text{V}$). Image taken 1 Å closer than the set point of $\Delta f =$ -0.7 Hz and $V = 0.4\,\text{V}$. Scale bar is 5 Å.

molecular orbital (LUMO) of the molecule is accessed and an electron from the tip is attached to DINP at about 1.85 V, as shown in Fig. 2 (a), creating an anion. By reversing the direction of the voltage sweep, the additional electron is detached from DINP to the tip at about 1.75 V, turning DINP neutral again. The difference of attachment and detachment energy is related to the reorganization energy. However, the stochastic nature of the tunneling process and the broadened energy levels cause a significant variation of the voltages of individual attachment and detachment events. A more elaborate and qualitatively different experiment is needed to quantify the attachment and detachment energies, as described recently [33]. The electron attachment/detachment cycle can be consecutively performed and indicates that the DINP anion is structurally stable on NaCl. Another proof of the DINP anion stability is the constant-height AFM image taken at 2.3 V (Fig. 1 (c)), when DINP is already singly negatively charged. The DINP cation is also stable (see supplemental material for details). The stability of the singly charged species suggests the possibility of using DINP as means to transfer single electrons and holes between such molecules [32, 34].

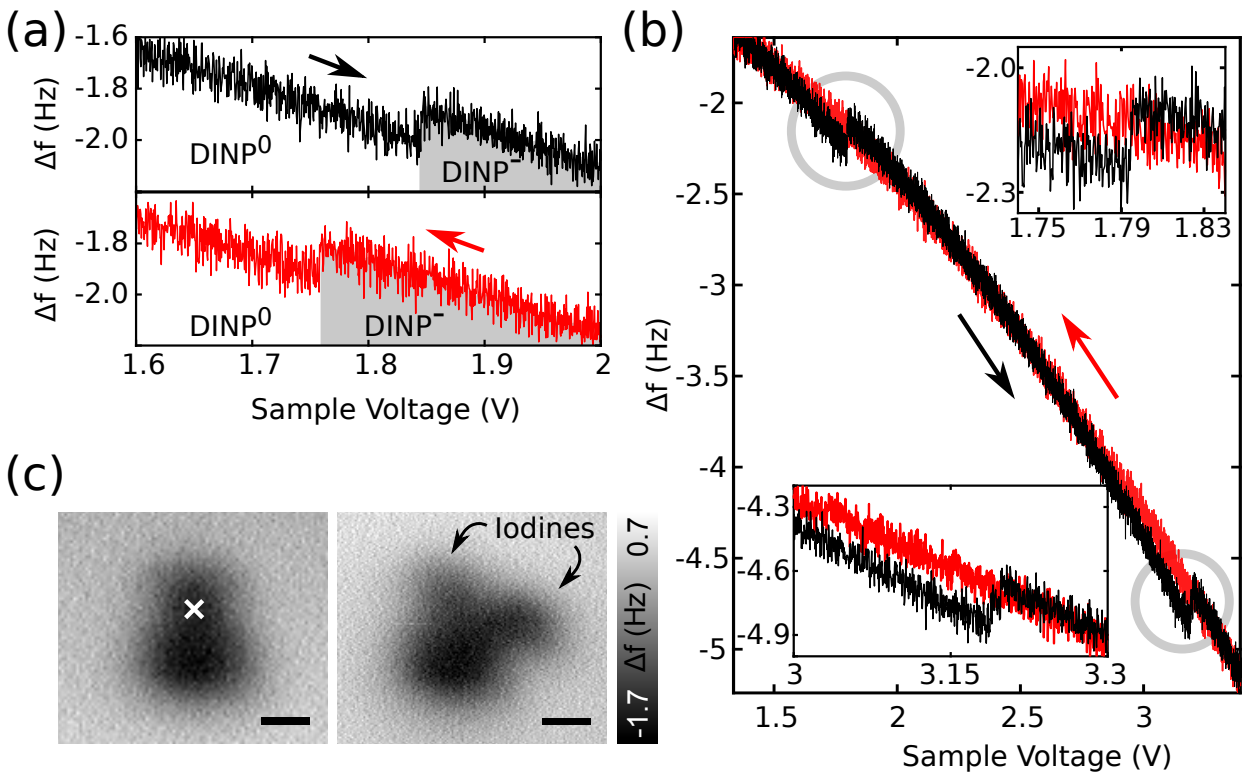


FIG. 2. (Color online) **(a)** $\Delta f\,(V)$ spectra on DINP for the reversible single-electron attachment (upper spectrum) and detachment (lower spectrum). **(b)** $\Delta f\,(V)$ spectrum for the double charging of DINP. Insets correspond to the magnified circled regions of the first and second electron attachment, respectively. Sample voltage sweep is from 1.3 V to 3.5 V (black trace). The reverse sweep is shown as a red trace. **(c)** Constant-height AFM images before (left, same as Fig. 1c) and after (right) attaching two electrons to DINP. Right image ($A = 4$ Å and $V = 2.4$ V) is taken 4 Å closer than the set point value of $\Delta f =$ - 0.7 Hz and $V = 0.4$ V. Scale bars are 5 Å.

The attachment of two electrons to DINP is shown in the $\Delta f\,(V)$ spectrum in Fig. 2 (b). At $V = 1.79$ V an electron is attached to the neutral DINP, similarly to Fig. 2 (a). By continuing ramping to higher positive sample voltages, at 3.17 V another step in the $\Delta f\,(V)$ spectrum is observed, signaling the attachment of the second electron to DINP. The increase in voltage for the attachment of the second electron compared to the first is related to the Coulomb repulsion energy. In stark contrast to the single-electron charging experiment (Fig. 2 (a)), the $\Delta f\,(V)$ spectrum is featureless when sweeping the sample voltage back to 0 V after attachment of the second electron (Fig. 2 (b)), i.e, steps in $\Delta f\,(V)$ indicating electron transfer are not observed. Constant-height AFM images taken before and after the

attachment of the second electron are shown in Fig. 2 (c). After doubly charging DINP, one large and two smaller rounded features are observed. The large feature corresponds to the hydrocarbon backbone of the molecule, i.e. the aryne [31]. The two smaller features are assigned to single iodines. Hence, by attaching two electrons to DINP, both iodines are dissociated from the molecule, yielding aryne and two separated iodines. The charge state of the products will be discussed below.

Next, the behavior of the fragmented units upon sweeping $V$ to negative values is investigated. After a neutral DINP (Fig. 3 (a)) is doubly negatively charged by sweeping to large positive $V$ (about 3.5 V), undergoing the fragmentation process (Fig. 3 (b)), $V$ is then swept to -1.5 V. The corresponding $\Delta f\,(V)$ spectrum shown in Fig. 3 (c) presents a step at -0.8 V. A constant-$\Delta f$ AFM image (Fig. 3 (d)) obtained after the spectrum evidences the same contrast as for the intact DINP before dissociation (Fig. 3 (a)). Hence, by sweeping to negative sample voltages, the iodines are reattached to aryne, forming DINP. In some cases, instead of one $\Delta f$ step, we can also observe two minor $\Delta f$ steps when the iodines are reattached (details in the supplemental material).

To prove the reversibility of the chemical reaction, a repeated voltage ramp is performed. First, two electrons are attached to DINP, by sweeping the sample voltage to 3.5 V. Afterwards, the sample voltage is swept to -1.5 V, leading to the reattachment of the iodines to aryne. Such sequence, sequentially executed three times, is shown in Fig. 3 (e) with the $\Delta f\,(t)$ and the corresponding $V(t)$ spectra, the steps in $\Delta f\,(t)$ indicate electron transfers and reactions as assigned in the individual voltage sweeps in Fig. 2 (b) and Fig. 3 (b). The constant-$\Delta f$ AFM images taken before and after the repeated sweep reveal identical contrasts for DINP proving that the molecule is reversibly dissociated (AFM images are shown in the supplemental material).

To elucidate the dissociation mechanism upon two-electron-attachment, a single iodine on NaCl is investigated (details in the supplemental material). The charge-state transitions are evaluated by the $\Delta f\,(V)$ spectrum with the tip above such an adatom. The upper panel in Fig. 4 (a) evidences that while sweeping from positive to negative sample voltages, a $\Delta f$ step occurs at around -1.4 V. Hence, the charge state of the iodine has changed. By reverting the sample voltage sweep, a $\Delta f$ step occurs at around -0.3 V, reverting to the initial charge state. This can be concluded because the $\Delta f\,(V)$ trace is the same as the initial $\Delta f\,(V)$ trace. No further $\Delta f$ transitions are measured from -2.5 V to 3 V (supplemental material). Because

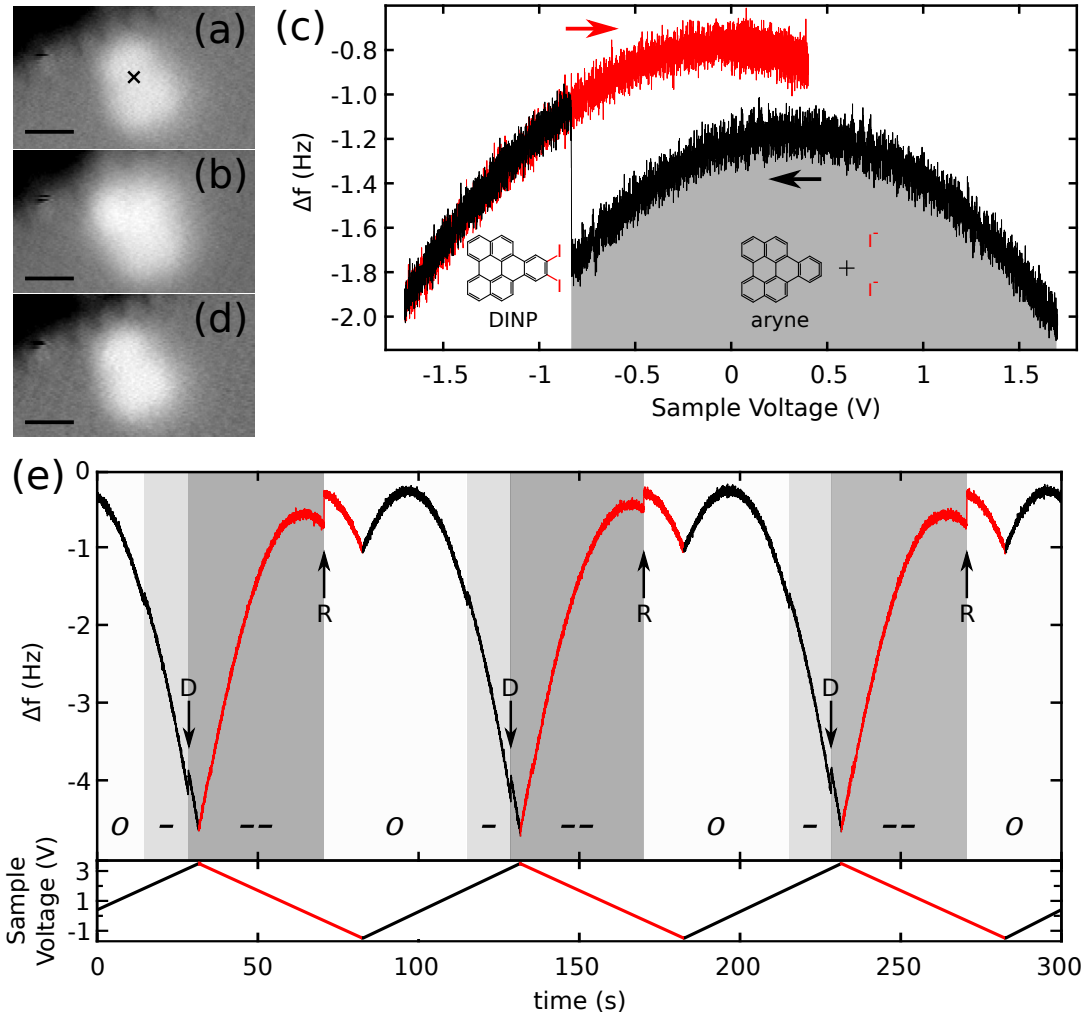


FIG. 3. (Color online) **(a, b, d)** Sequential constant–$\Delta f$ images of **(a)** DINP prior dissociation, **(b)** dissociated DINP after two-electron attachment and before the spectrum in **(c)** was performed and **(d)** after performing the spectrum in **(c)**. Image set points are the same ($\Delta f$ = -0.5 Hz and $V$ = 0.4 V) and $A$ = 6 Å. Scale bars are 10 Å. **(c)** $\Delta f\,(V)$ spectra on aryne and iodines. The $V$ sweep starts from 1.7 V above the dissociated DINP. First $V$ is swept to -1.7 V (black trace). The reverse sweep is shown as a red trace and ends at 0.4 V. **(e)** $\Delta f$ (t) spectrum of consecutive sample voltage ramps above DINP. The dissociation (D) and restoration (R) of the C-I bonds are indicated in the spectrum. The different total charge-states of the system are indicated by gray levels in the image. The system is composed of DINP, while neutral and negatively charged, and aryne plus two iodines after being doubly negatively charged. Black trace corresponds to sample voltage sweeps from negative to positive values, whereas the red trace corresponds to the opposite. Constant-$\Delta f$ images of DINP before and after the spectrum in **(e)** are included in the supplemental material.

of the large ionization energy of an iodine (10.5 eV) the switching to the positive charge state can be ruled out. Moreover, the electron affinity of iodine is large (3.5 eV) [35, 36]. Therefore, we assign the observed charge state transitions of iodine to transitions between the negative and neutral charge state.

DFT calculations were performed using the FHI-AIMS code [37]. Each one of the possible charged components, aryne and iodine, was independently investigated on a 4 layer thick NaCl slab composed of 256 atoms. The geometry of the given system was optimized with the *tight* basis defaults. For structural relaxation, the Perdew-Burke-Ernzerhof exchange-correlation functional was applied [38] with vdW correction [39]. The convergence criteria for the total forces was $10^{-3}$ eV/Å and for the total energy it was set to $10^{-5}$ eV. The calculations of the total energies of the different products (aryne and iodines) with different charge configurations (0, $-1$ and $-2$), plotted in Fig. 4 (b), show that the configuration with a neutral aryne and two negatively charged iodines (iodides) has the lowest total energy for a system whose total charge configuration is two electrons. The closest charge-state configuration in energy is the doubly negatively charged DINP, almost 1 eV higher in energy.

Based on the experimental evidence of the necessary number of additional electrons for the dissociation to take place and the insight gained with the DFT calculations, the most feasible mechanism is that of Coulombic explosion [40, 41]. After attaching two electrons to DINP, the dissociation takes place to reduce the Coulomb repulsion. In contrast to the Au-PTCDA switch on bilayer NaCl [42], different charge-states on thicker insulating films are long-lived because of the decoupling from the metal substrate by the multilayer insulating film and do not necessarily require stabilization by ionic relaxations in the film [2, 43, 44]. Another important point is that the total charge-state of the complex can be precisely inferred by following the $\Delta f\,(V)$ spectra. The experiment shows also that reformation of the iodine bonds occurs by charging. In contrast to the dissociation, only a single $\Delta f\,(V)$ step is observed, indicating that two electrons are removed at this specific voltage. The repeated dissociation of DINP after its restoration evidences that it becomes neutralized in the $\Delta f\,(V)$ step associated with the DINP reformation. The bond reformation could be explained by the following tentatively assigned mechanism: When we reach the HOMO of the aryne in the negative voltage sweep, it gets singly positively charged. This leads, on time scales that are much faster than our AFM's time resolution (about 0.1 s) to the following cascade of events: First, upon charging the aryne positively an iodide attacks aryne forming

a C-I bond. This leads to a neutral iodonaphthoperylene (INP) radical. Second, the INP HOMO (due to the uneven number of electrons it is a singly occupied molecular orbital) is expected at even higher energies compared to the aryne's HOMO, thus the radical gets quickly charged positively again at the voltage applied. Third, the positive charge of the radical triggers the attack of the second iodide to form another C-I bond leading to a neutral DINP molecule. Comparison with the measurements on individual iodine/iodide rule out the neutralization of the iodides by hole attachment at voltages larger than -1 V. Moreover, charging the aryne doubly positive before the iodines are reattached would result in two well separated $\Delta f$ steps for the charging events at different voltage, because of Coulomb repulsion. The reaction pathways for different charge states are summarized in Fig. 4 (c).

To conclude, we demonstrated molecular bond dissociation and formation by atomic manipulation on an insulator by employing dianionic charge states. The system was investigated by AFM with the charge-state changes of the reactant being surveyed with Kelvin probe force spectroscopy. By attaching two electrons to the molecule, the fragmentation occurred. The high yield of this process based on the attachment of two long-lived electrons is attributed to the breaking of the halogen-carbon bond as a result of the Coulomb repulsion. Furthermore, the halogen-carbon bonds could be consistently reformed by what is tentatively assigned to Coulomb attraction. The molecule studied here is exemplary of molecular systems where the transfer of a single charge is stable, but further addition of charges result in induced chemical reactions. Thus, such systems can be employed to both transfer charge between molecules by electron hopping [32] and to induce reversibly chemical reactions by charge attachment.

We thank Rolf Allenspach, Niko Pavliček, Zsolt Majzik and Fabian Schulz for comments. We thank the European Research Council (Advanced grant 'CEMAS', agreement No. 291194 and Consolidator grant 'AMSEL', agreement No. 682144), EU projects 'PAMS' (Contract No. 610446) and the Initial Training Network 'ACRITAS' (Contract No. 317348), the Spanish Ministry of Economy and Competitiveness (projects MAT2016-78293-C6-3R and CTQ2016-78157-R), Xunta de Galicia (Centro Singular de Investigacíon de Galicia accreditation 2016-2019, ED431G/09) and the European Union (European Regional Development Fund - ERDF) for the financial support.

* shadikeitaro@gmail.com

† lgr@zurich.ibm.com

[1] W. Ho, Accounts of Chemical Research **31**, 567 (1998).

[2] J. Repp, G. Meyer, S. Paavilainen, F. E. Olsson, and M. Persson, Science **312**, 1196 (2006).

[3] R. Lindner and A. Kühnle, ChemPhysChem **16**, 1582 (2015).

[4] N. Pavliček and L. Gross, Nature Reviews Chemistry **1**, 0005 (2017).

[5] S.-W. Hla, L. Bartels, G. Meyer, and K.-H. Rieder, Physical Review Letters **85**, 2777 (2000).

[6] H. Lee and W. Ho, Science **286**, 1719 (1999).

[7] L. J. Lauhon and W. Ho, The Journal of Physical Chemistry A **104**, 2463 (2000).

[8] J. K. Gimzewski and C. Joachim, Science **283**, 1683 (1999).

[9] L. Bartels, G. Meyer, and K.-H. Rieder, Physical Review Letters **79**, 697 (1997).

[10] T. A. Jung, R. R. Schlittler, J. K. Gimzewski, H. Tang, and C. Joachim, Science **271**, 181 (1996).

[11] G. Dujardin, R. E. Walkup, and P. Avouris, Science **255**, 1232 (1992).

[12] B. C. Stipe, M. A. Rezaei, W. Ho, S. Gao, M. Persson, and B. I. Lundqvist, Physical Review Letters **78**, 4410 (1997).

[13] P. A. Sloan and R. E. Palmer, Nature **434**, 367 (2005).

[14] B. Schuler, S. Fatayer, F. Mohn, N. Moll, N. Pavliček, G. Meyer, D. Peña, and L. Gross, Nature Chemistry **8**, 220 (2016).

[15] N. Pavliček, A. Mistry, Z. Majzik, N. Moll, G. Meyer, D. J. Fox, and L. Gross, Nature Nanotechnology **12**, 308 (2017).

[16] W. Steurer, L. Gross, and G. Meyer, Applied Physics Letters **104**, 231606 (2014).

[17] M. Abel, S. Clair, O. Ourdjini, M. Mossoyan, and L. Porte, Journal of the American Chemical Society **133**, 1203 (2011).

[18] R. Lindner, P. Rahe, M. Kittelmann, A. Gourdon, R. Bechstein, and A. Kühnle, Angewandte Chemie International Edition **53**, 7952 (2014).

[19] M. Kittelmann, P. Rahe, M. Nimmrich, C. M. Hauke, A. Gourdon, and A. Kühnle, ACS Nano **5**, 8420 (2011).

[20] T. Dienel, J. Gómez-Díaz, A. P. Seitsonen, R. Widmer, M. Iannuzzi, K. Radican, H. Sachdev,

K. Müllen, J. Hutter, and O. Gröning, ACS Nano **8**, 6571 (2014).

[21] F. Para, F. Bocquet, L. Nony, C. Loppacher, M. Féron, F. Cherioux, D. Z. Gao, F. F. Canova, and M. B. Watkins, Nature Chemistry , 1 (2018).

[22] L. Gross, F. Mohn, P. Liljeroth, J. Repp, F. J. Giessibl, and G. Meyer, Science **324**, 1428 (2009).

[23] Y. Sugimoto, M. Abe, S. Hirayama, N. Oyabu, Ó. Custance, and S. Morita, Nature Materials **4**, 156 (2005).

[24] Y. Sugimoto, P. Pou, O. Custance, P. Jelinek, M. Abe, R. Perez, and S. Morita, Science **322**, 413 (2008).

[25] S. Kawai, A. S. Foster, F. F. Canova, H. Onodera, S.-i. Kitamura, and E. Meyer, Nature Communications **5**, 4403 (2014).

[26] R. Stomp, Y. Miyahara, S. Schaer, Q. Sun, H. Guo, P. Grutter, S. Studenikin, P. Poole, and A. Sachrajda, Physical Review Letters **94**, 056802 (2005).

[27] E. Bussmann and C. C. Williams, Applied Physics Letters **88**, 263108 (2006).

[28] F. J. Giessibl, Applied Physics Letters **73**, 3956 (1998).

[29] T. Albrecht, P. Grütter, D. Horne, and D. Rugar, Journal of Applied Physics **69**, 668 (1991).

[30] L. Gross, F. Mohn, N. Moll, P. Liljeroth, and G. Meyer, Science **325**, 1110 (2009).

[31] N. Pavliček, B. Schuler, S. Collazos, N. Moll, D. Pérez, E. Guitián, G. Meyer, D. Peña, and L. Gross, Nature Chemistry **7**, 623 (2015).

[32] W. Steurer, S. Fatayer, L. Gross, and G. Meyer, Nature Communications **6**, 8353 (2015).

[33] S. Fatayer, B. Schuler, W. Steurer, I. Scivetti, J. Repp, L. Gross, M. Persson, and G. Meyer, Nature Nanotechnology **13**, 376 (2018).

[34] P. Rahe, R. P. Steele, and C. C. Williams, Nano Letters **16**, 911 (2016).

[35] D. Hanstorp and M. Gustafsson, Journal of Physics B: Atomic, Molecular and Optical Physics **25**, 1773 (1992).

[36] D. R. Lide, ed., *CRC Handbook of Chemistry and Physics* (CRC Press; 90 edition, 2009).

[37] V. Blum, R. Gehrke, F. Hanke, P. Havu, V. Havu, X. Ren, K. Reuter, and M. Scheffler, Computer Physics Communications **180**, 2175 (2009).

[38] J. P. Perdew, K. Burke, and M. Ernzerhof, Physical Review Letters **77**, 3865 (1996).

[39] A. Tkatchenko and M. Scheffler, Physical Review Letters **102**, 073005 (2009).

[40] T. A. Carlson and R. M. White, The Journal of Chemical Physics **44**, 4510 (1966).

[41] J. H. D. Eland, R. Singh, J. D. Pickering, C. S. Slater, A. H. Roos, J. Andersson, S. Zagorodskikh, R. J. Squibb, M. Brouard, and R. Feifel, The Journal of Chemical Physics **145**, 074303 (2016).

[42] F. Mohn, J. Repp, L. Gross, G. Meyer, M. S. Dyer, and M. Persson, Physical Review Letters **105**, 266102 (2010).

[43] F. E. Olsson, S. Paavilainen, M. Persson, J. Repp, and G. Meyer, Physical Review Letters **98**, 176803 (2007).

[44] J. Repp, W. Steurer, I. Scivetti, M. Persson, L. Gross, and G. Meyer, Physical Review Letters **117**, 146102 (2016).

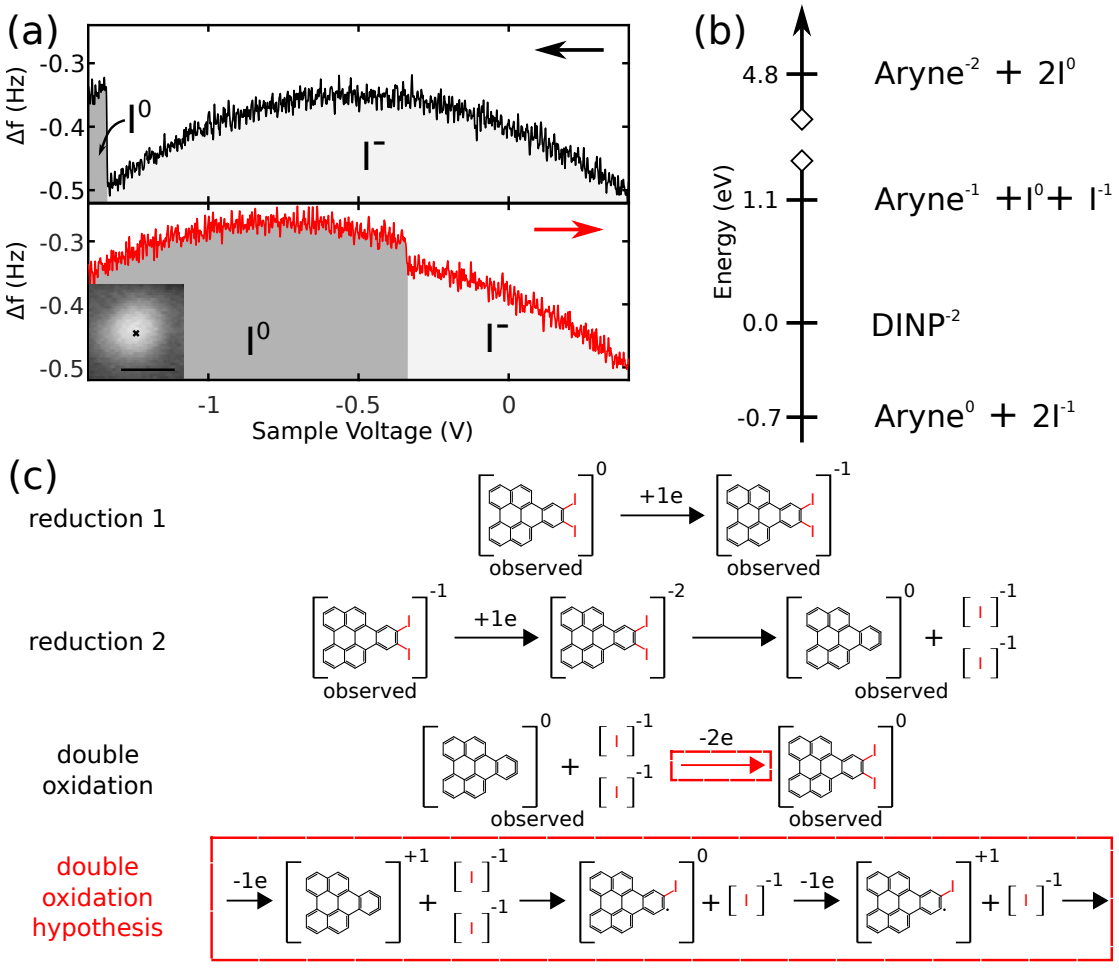


FIG. 4. (Color online) **(a)** $\Delta f\,(V)$ spectra on top of a single iodine. From positive to negative sample voltage (upper panel) and the reverse sweep (lower panel). The inset displays a constant-$\Delta f$ image of an iodide ($\Delta f$ = -0.7 Hz, $V = 0.4$ V and $A = 6$ Å) with a scale bar of 5 Å. Black and white scale ranges from 0 Å to 2.3 Å. **(b)** Calculated total energies for different chemical products with varied charge-state configurations on top of NaCl. **(c)** Reaction pathways for different charge states. First, the stability of DINP upon single electron attachment. Second, the fragmentation of the anionic DINP upon electron attachment. Third, the C-I bond restoration upon doubly charging aryne and two iodines. Fourth, the C-I restoration hypothesis where the aryne gets positively charged, then, an iodide attacks the positively charged aryne forming INP. Without the need to further decrease the voltage, INP gets positively charged. Finally, another iodide attacks the positively charged INP, forming DINP.

# Supplemental Material

# Controlled fragmentation of single molecules by employing doubly charged states with atomic force microscopy

Shadi Fatayer,[1,*] Nikolaj Moll,[1] Sara Collazos,[2] Dolores Pérez,[2]
Enrique Guitián,[2] Diego Peña,[2] Leo Gross,[1] and Gerhard Meyer[1]

[1]*IBM Research – Zurich, Säumerstrasse 4, 8803 Rüschlikon, Switzerland*

[2]*Centro de Investigación en Química Biolóxica e Materiais Moleculares (CIQUS) and Departamento de Química Orgánica, Universidade de Santiago de Compostela, Santiago de Compostela 15782, Spain*

(Dated: July 18, 2018)

PACS numbers: 68.37.Ps, 68.35.-p, 68.43.-h, 82.30.Qt, 82.37.Gk

## DINP CATION AND DICATION STABILITY

In Fig. 1 we show that the DINP is stable in the singly and doubly positively charged states. This is showcased by reversibly attaching one and two holes to DINP, respectively.

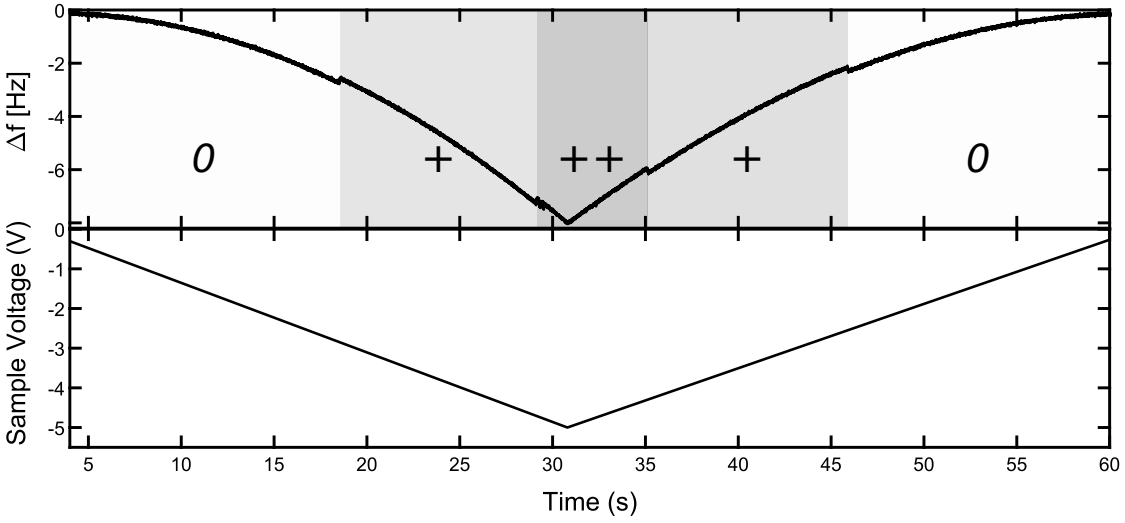


FIG. 1. $\Delta f\,(V)$ spectroscopy. $V$ is swept from -0.2 V to -5 V. $\Delta f$ (upper panel) and $V$ (lower panel) are shown as a function of time on DINP for sequential hole attachments and detachment.

## PRODUCTS COMPARISON BY DIFFERENCE IN AFM IMAGES

We compare the differences between AFM images of pristine DINP, shown in Fig. 2 (a), with AFM images of DINP after being doubly charged, shown in Fig. 2 (b). The difference image, obtained by subtracting the AFM images is shown in Fig. 2 (d). It evidences two lobes which we assign to the iodines that were dissociated from the molecule. An inverted contrast (Fig. 2 (e)) is obtained in the difference image when comparing an AFM image of the restored DINP upon two-holes attachment, Fig. 2 (c), with an AFM image of the fragmented DINP molecule, Fig. 2 (b). The absence of noticeable contrast between AFM images Fig. 2 (c) and Fig. 2 (a) shown as difference images in Fig. 2 (f) further demonstrates that the DINP molecule is intact upon two-hole attachment.

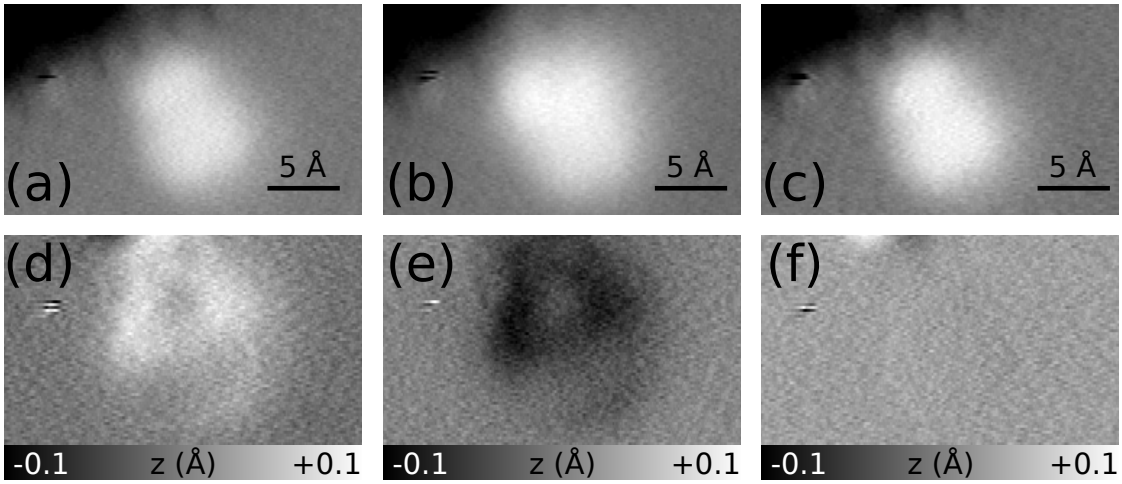


FIG. 2. **(a–c)** Sequential constant-$\Delta f$ images of **(a)** DINP, **(b)** dissociated DINP after attachment of two electrons and **(c)** after performing the spectrum in Fig. 3c of the main article. Set points in the images are the same ($\Delta f$ = -0.5 Hz and $V = 0.4$ V). The images are the same as in Fig. 3b–d in the main article. The scale in the images range from 0 (black) to 10 Å (white). **(d)** Difference image between (b) and (a). **(e)** Difference image between (c) and (b). **(f)** Image difference between (c) and (a).

## DOUBLE $\Delta F$ STEPS UPON C-I REFORMATION

As stated in the main text, sweeping the sample voltage to negative values while the tip is on top of a dissociated DINP, there are two $\Delta f$ behaviors observed. A single $\Delta f$ step, as shown in Fig. 3c of the main text, is observed in most cases. In some cases there are two consecutive $\Delta f$ steps observed, as shown in Fig. 3. Both behaviors yield the same result - the $\Delta f$ parabola is the same as of the neutral DINP.

## SPECTROSCOPY ON IODINES

A single iodine is investigated in Fig. 4 by performing a $\Delta f$ (V) spectrum. The iodine is obtained in the fragmentation process of DINP. Sometimes the iodines move away from aryne by several NaCl lattice constants, preventing the C-I bond restoration. By placing the tip on top of the iodines and charging them, they may move. With such procedure, we isolated the iodines. From the fragmented molecules, approximately 50% have one of the iodines moving further away, such that the C-I bond restoration cannot be established. The average center-

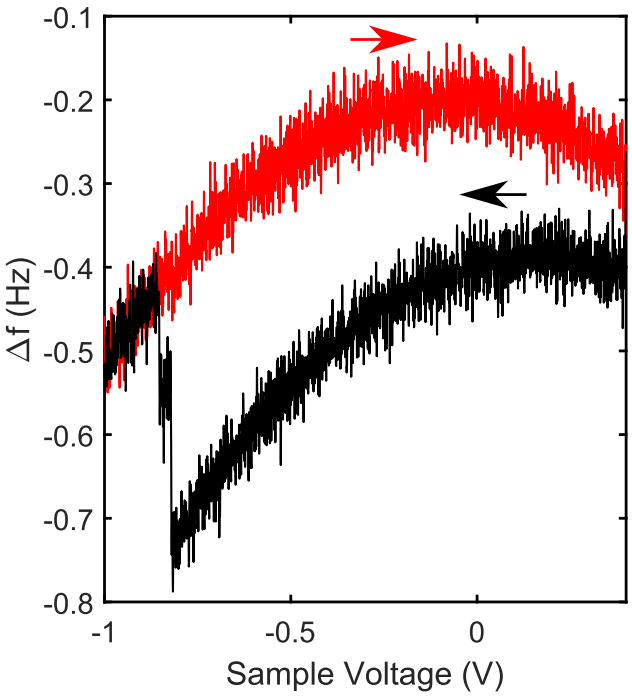


FIG. 3. $\Delta f\,(V)$ spectra on aryne and iodines. The voltage sweep starts from 0.4 V and goes to -1 V (black trace). The reverse sweep is shown as a red trace.

to-center distance between iodines and the center of aryne is then approximately 11 Å or larger. The average center-to-center distance between iodines and aryne for the molecules that we managed to restored is approximately 9 Å.

## DISCUSSION ABOUT CHARGE-STATE TRANSITION DISCERNMENT

The main characteristic used in discerning a charge-state transition is the difference between $\Delta f\ (V)$ for distinct charge states of an adsorbate. For charge-state transitions where there is visible difference in this value (meaning a larger $\Delta f$ difference than the noise in the $\Delta f$ ), a charge-state transition is observed as a step in the $\Delta f\,(V)$ spectrum. If this condition is not encountered, a charge-state transition can still be evaluated by comparing the resulting parabolas. This is an effect of the local contact potential difference change due to charging of the adsorbate. Whether a charge-state transition is clearly observed as a $\Delta f$ step will depend on the tip geometry and more importantly on how large is the absolute voltage difference between the local contact potential difference and the voltage for which the charge-state transition has occurred. As an example, we highlight Fig. 4 where the

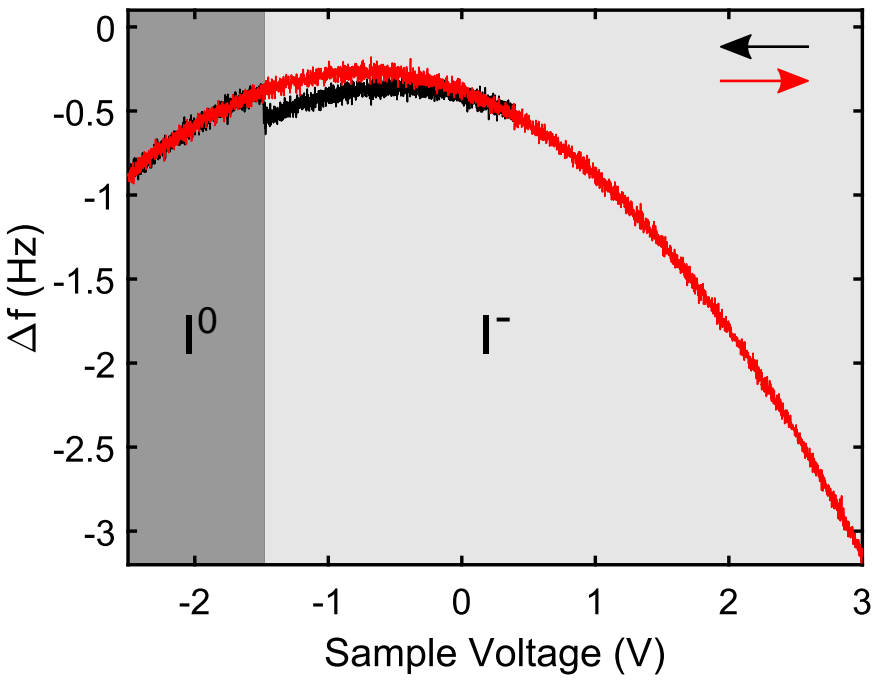


FIG. 4. $\Delta f\ (V)$ spectra on top of a single iodine. Black trace goes from positive (0.4 V) to negative sample voltages (-2.5 V). Red trace goes from negative (-2.5 V) to positive (+3.0 V) sample voltages.

$I^{-1} \rightarrow I^0$ transition is clearly observed at approximately -1.5 V but the opposite charge state transition cannot be pinpointed by a $\Delta f$ step. However, after 0 V the red and the black traces appear to follow the same parabola, meaning that the $I^0 \rightarrow I^{-1}$ has occurred. A spectrum performed with reduced sample voltage speed, as seen in Fig. 4(a) of the main article, clearly depicts both charge-state transitions.

## SLIGHT ADSORBATE MOVEMENT UPON CONSECUTIVE BREAKING AND FORMING OF C-I BONDS

We note that in the $\Delta f$ spectra for DINP in Fig. 3e of the main manuscript, another step, smaller in height than the step corresponding to a molecular charge-state transition, is observed at around 3.1 V (such $\Delta f$ step appears at times 35 s, 135 s and 236 s in Fig. 3e) while sweeping the sample voltage to negative values. We attribute this step to a slight movement of the adsorbates. After consecutively fragmenting and reestablishing the iodine bonds three times, DINP translated closer to the NaCl step edge. This is demonstrated

by comparing AFM images before (Fig. 5 (a)) and after (Fig. 5 (b)) the $\Delta f$ spectrum with consecutive voltage ramps in the main text.

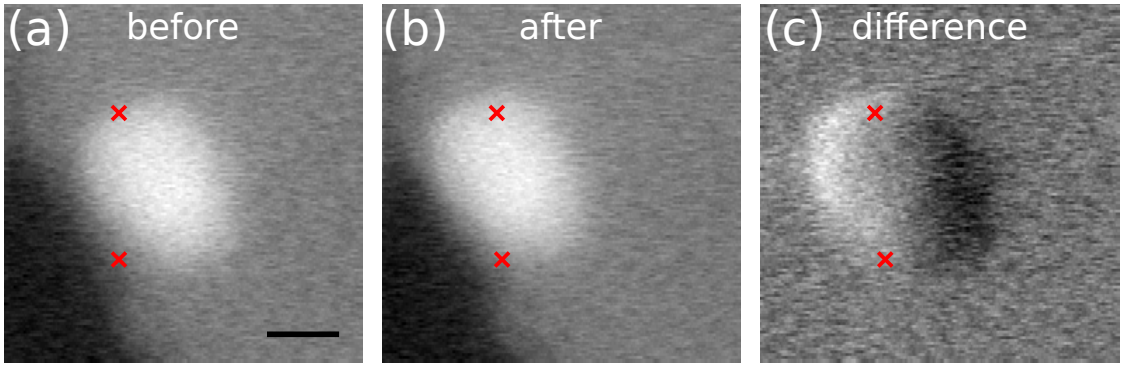


FIG. 5. **(a–c)** Sequential constant-$\Delta f$ images of DINP before **(a)** and after **(b)** consecutively dissociating and reforming the I-C bonds in the spectrum shown in Fig. 3e of the main article. Set points in the images are the same ($\Delta f$ = -0.3 Hz and $V = 0.4$ V). Scale bar is 10 Å. Red crosses are drawn as a guide to the eye marking fixed positions in the image frame. **(c)** Difference image between **(b)** and **(a)**, showcasing a lateral movement of the molecule to the left-hand side.

In Fig. 6 we show a $\Delta f$ (t) spectrum of the fragmentation of DINP without such additional $\Delta f$ step. Two steps in $\Delta f$ are observed, each indicating a single-electron transfer to the molecule.

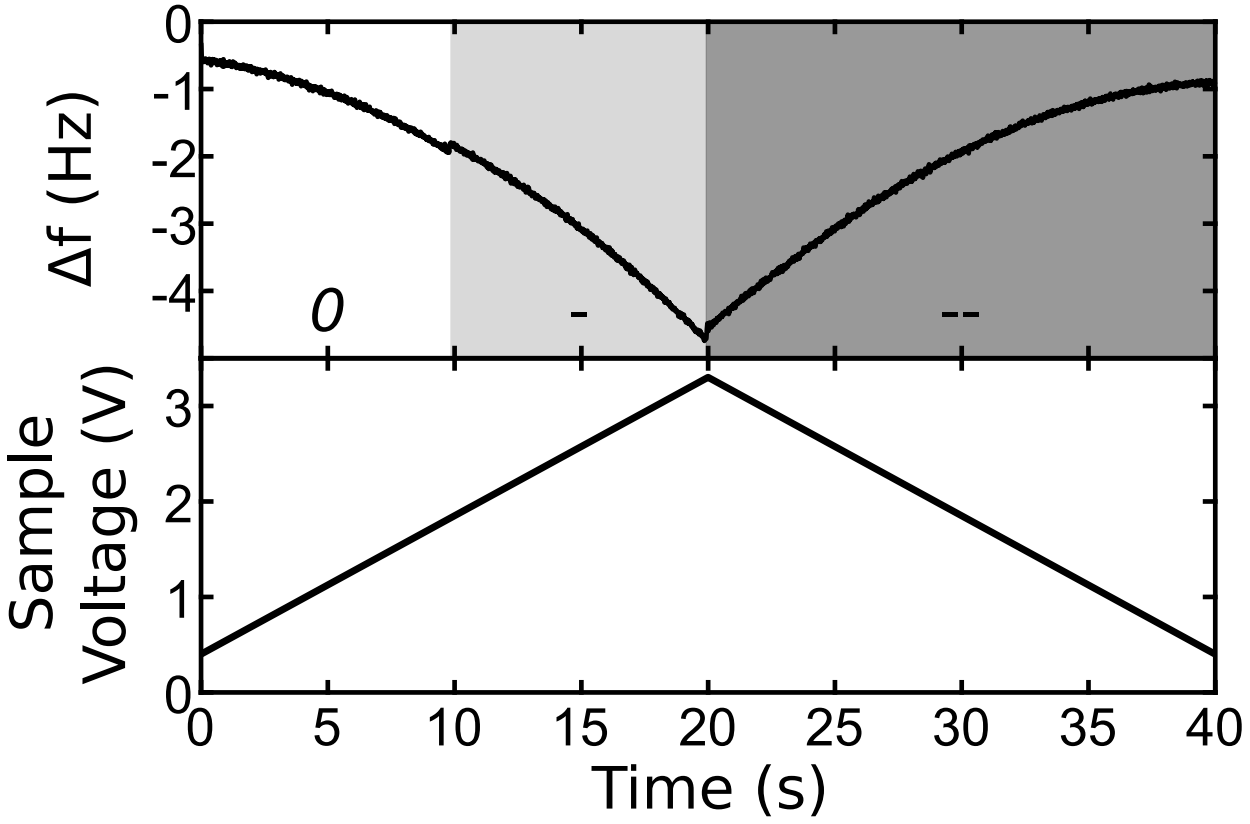


FIG. 6. $\Delta f$ (t) spectrum of consecutive electron attachment to DINP.